Geophysical Research Letters

RESEARCH LETTER
10.1029/2021GL094179

Key Points:

- The operational rainfall forecasts during the summer of 2020 considerably underestimated the observed amount over East Asia
- The heavy rainfall over East Asia during 2020 summer is successfully predicted in GloSea5 by correcting tropical SST forcing
- The quality of simulated climatological SST fields impact the operational seasonal forecast skill

Supporting Information:

Supporting Information may be found in the online version of this article.

Correspondence to:

Y.-G. Ham,
ygham@jnu.ac.kr

Citation:

Ham, Y.-G., Kim, J.-G., Lee, J.-G., Li, T., Lee, M.-I., Son, S.-W., & Hyun, Y.-K. (2021). The origin of systematic forecast errors of extreme 2020 East Asian summer monsoon rainfall in GloSea5. *Geophysical Research Letters*, *48*, e2021GL094179. https://doi.org/10.1029/2021GL094179

Received 3 MAY 2021
Accepted 10 AUG 2021

The Origin of Systematic Forecast Errors of Extreme 2020 East Asian Summer Monsoon Rainfall in GloSea5

Yoo-Geun Ham[1], Ji-Gwang Kim[1], Jeong-Gil Lee[1], Tim Li[2,3], Myong-In Lee[4], Seok-Woo Son[5], and Yu-Kyung Hyun[6]

[1]Department of Oceanography, Chonnam National University, Gwangju, South Korea, [2]International Pacific Research Center (IPRC), and Department of Atmospheric Sciences, SOEST, University of Hawaii at Manoa, Honolulu, HI, USA, [3]Ministry of Education/Joint International Research Laboratory of Climate and Environmental Change/Collaborative Innovation Center on Forecast and Evaluation of Meteorological Disasters, Nanjing University of Information Science and Technology (NUIST), Nanjing, China, [4]Department of Urban and Environmental Engineering, Ulsan National Institute of Science and Technology, Ulsan, South Korea, [5]School of Earth and Environmental Sciences, Seoul National University, Seoul, South Korea, [6]Operational Systems Development Department, National Institute of Meteorological Sciences, Jeju, South Korea

Abstract This study examined the origin of the systematic underestimation of rainfall anomalies over East Asia during July–August 2020 in operational forecasts. Through partial nudging experiments, we found that the East Asian rainfall anomalies were successfully predicted in GloSea5 with corrected tropical sea surface temperature (SST) forcing. Once the observed SST is applied over the Indian Ocean and tropical central-eastern Pacific, a low-level anticyclonic anomaly over the subtropical western Pacific, which transports warm-moist air from the tropics to increase the East Asian precipitation, is well reproduced as observed. By further separating the SST into climatological and anomalous components, we revealed that the cold and dry mean state bias over the Indian Ocean and central-eastern Pacific is responsible for the weak anomalous atmospheric teleconnection patterns from the tropics to East Asia. This implies that correcting the model mean climatological fields can directly impact the operational seasonal forecast skill.

Plain Language Summary Adapting to destructive climate events based on successful forecasts is one way to reduce social and economic losses. Unfortunately, the operational rainfall forecasts during the summer of 2020 systematically underestimated the amount of rainfall anomalies over East Asia. Through partial nudging experiments, we found that East Asian rainfall anomalies were successfully predicted by correcting the tropical sea surface temperature (SST) forcing in the operational forecast system. The development of the anticyclonic flow anomalies over the subtropical western Pacific, which transport warm and wet air from the tropics and increase East Asian precipitation, could be accurately predicted once the observed SST is prescribed over the Indian Ocean and tropical central eastern Pacific in operational seasonal forecast system.

1. Introduction

During the summer of 2020, a large amount of rainfall was recorded over East Asia, including Korea, Japan, and China (Pan et al., 2021; Zhang et al., 2021). In particular, Korea suffered a series of heavy rainfall events from early July to mid August, 2020 (C. Park et al., 2021). The amount of rainfall accumulated from July 1 to August 12, 2020 over South Korea is 162% larger than the climatological amount, and exhibits a second highest amount in recent 40 years (Figure 1a). As a result, East Asian countries suffered a destructive floods caused severe economic losses and casualties in 2020 summer.

Adapting to destructive climate events based on successful forecasts is one way to reduce social and economic losses. However, it was unfortunate that the operational rainfall forecasts during the summer of 2020 using Global Seasonal forecast system version 5 (GloSea5, MacLachlan et al., 2015) systematically underestimated the amount of rainfall anomalies over East Asia. The forecasted rainfall anomalies from July 1 to August 12, 2020 by the ensemble forecast initialized at June 1 is nearly zero (Figure 1b).

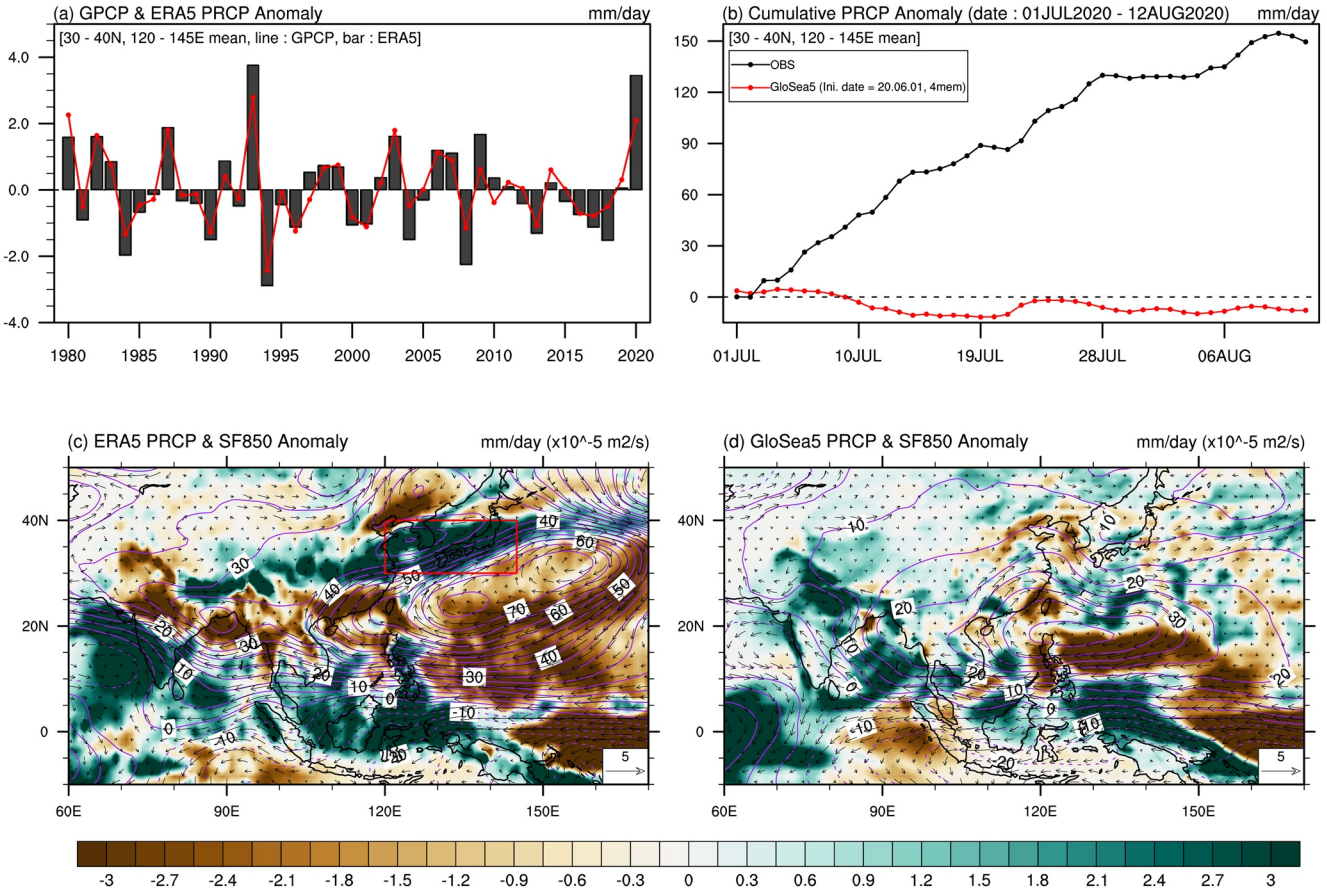

Figure 1. (a) Area-averaged (30°–40°N, 120°–145°) (e) precipitation anomalies during July 1–August 12 in the observation from 1980 to 2020 using ERA5 (black bar) and GPCP version 2 (red line). (b) Cumulative precipitation of the observed (black) and GloSea5 predictions (red) over Korea, Japan region (30°–40°N, 120°–145° (e) from July 1 to August 12, 2020. (c) Observed precipitation anomaly (shaded), 850 hPa streamfunction (contour), and 850 hPa wind-vector. (d) GloSea5-predicted precipitation anomaly (shaded), 850 hPa stream function (contour), and 850 hPa wind vector averaged from July 1 to August 12, 2020. Note that the GloSea5 forecasts are initialized at June 1, 2020.

The successful real-time forecasts of the record-breaking summer rainfall in 2020 over East Asia were quite challenging; however, through the post-analysis, the physical mechanisms of these rainfall events are partly understood. The large-scale anticyclonic flow over the western North Pacific (WNP) is closely associated with heavy rainfall over East Asia by advecting warm and moist air along the northwestern part of the anticyclone. The horizontal warm and moist air advection is compensated by the negative vertical moist energy advection by the upward motion, which condense the water vapor to increase the precipitation amount (Ham et al., 2007). The robust warm sea surface temperature (SST) over the Indian Ocean (IO), which is a typical time-delayed response to El Niño during the winter of 2019/20, is believed to be the primary cause of the large-scale anticyclone flow through the IO capacitor effect (Kosaka et al., 2013; E. J. Lee et al., 2006; Wu et al., 2009; Xie et al., 2009). In addition, SST anomalies in the tropical Pacific and Atlantic also play a role (T. Li et al., 2017; Wu et al., 2010).

The SST anomalies over the equatorial Pacific in 2020 might have also contributed to positive precipitation anomalies over East Asia (Pan et al., 2021). This is consistent with previous studies documenting that an anomalous low-level anticyclone over the WNP tends to develop during the decaying El Niño summer through a positive feedback maintained by the atmosphere-ocean coupling process (Wang & Zhang, 2002; Wang et al., 2003) and atmospheric moist entropy advection process (Wu et al., 2017a, 2017b).

Based on the relationship between the large-scale equatorial SST forcing and precipitation over East Asia, it can be speculated that the forecast errors in the tropical SST anomalies might be largely responsible for the forecast errors in the precipitation amount over East Asia. However, the amplitude and spatial distribution

of large-scale SST anomalies over the Indo-Pacific regions were reasonably predicted in 2020 summer (Figure S1). It makes the underlying mechanism leading to forecast errors over East Asia in the summer of 2020 unclear. Here, we conducted sensitivity experiments using Glosea5, the operational forecast system of the Korea Meteorological Administration (KMA; S. J. Lee et al., 2020; S. Park et al., 2017), to investigate the cause of systematic errors in predicting extreme precipitation over East Asia in the summer of 2020.

In Section 2, descriptions of the observational data and coupled (ocean-atmosphere) general circulation model (CGCM) used in this study are provided. The distinct roles of the NTA SST and Atlantic Niño are shown in section 3. Summary and conclusions are presented in sect

2. Data and Experimental Design

2.1. GloSea5 Hindcast and Observation

The GloSea5 hindcast data set that started on June 1, 2020 is utilized. The GloSea5 system consists of the Met Office Unified Model for the atmospheric component, Nucleus for European Modeling of the Ocean for oceanic components, Los Alamos sea ice model for the sea ice component, and Joint UK Land Environment Simulator for land components. The horizontal resolution was 0.83° (in longitudinal direction) × 0.56° (in latitudinal direction) and the number of vertical levels was 85 for the atmospheric component, and 0.25° × 0.25° with 75 vertical levels for the oceanic component (MacLachlan et al., 2015). For each hindcast, and operational forecast, three, and four ensemble members were generated using the stochastic physics scheme, respectively (Bowler et al., 2009). The model climatology is defined by averaging the hindcast experiments from 1991 to 2016, and the anomaly for year 2020 is computed by subtracting the climatological model fields from the forecast results in 2020.

To evaluate the forecast skill in 2020 summer, multiple observational data set are utilized. For SST, Optimum Interpolation SST version 2 from the NOAA was used (Reynolds et al., 2007). The precipitation, zonal and meridional winds were obtained from ERA5 from ECMWF (Hersbach et al., 2020). The monthly-mean Global Precipitation Climatology Project (GPCP) version 2 data set is also utilized (Adler et al., 2003). The data period spans from 1991 to 2016 and was set to be the same as the hindcast data set.

2.2. Partial Nudging Experiments

Partial nudging experiments were conducted using the GloSea5 to examine the atmospheric response to tropical SST forcing (Chikamoto et al., 2016; Ham et al., 2013, 2017). The initial condition is identical to that for the operational GloSea5 forecasts starting on June 1, 2020. The model was integrated from June 1 to August 12, 2020 by nudging SST with a relaxation time-scale of one hour. For the partial nudging experiments, the SST is applied over 20°S–20° N, 40°–100°E for the IO, and over 20° S–20° N, 180°–75° W for the equatorial eastern-central Pacific. The prescribed SST is a daily averaged value. A total of nine ensemble members are generated using a stochastic physics scheme (Bowler et al., 2009), and the ensemble-averaged values were analyzed as the response to the given SST.

To calculate the simulated anomalies in 2020, control experiments were conducted using the daily climatological SST fields, which is defined by averaging data from 1991 to 2020 at a corresponding day. All analyses are conducted for the results averaged from July 1 to August 12, when Korea suffered a series of intensive rainfall events (C. Park et al., 2021), unless otherwise mentioned.

3. Operational GloSea5 Forecast and Partial Nudging Experiments

Figures 1c and 1d show the spatial distribution of the observed, and simulated precipitation anomalies averaged from July 1 to August 12, 2020, respectively. The streamfunction and wind-vector anomalies at 850 hPa are also displayed. Robust positive precipitation anomalies are exhibited over East Asia, including Korea, Japan, and northern China. This prominent rainband covering Korea, Japan, and northern China is located over the northwestern edge of anticyclonic streamfunction anomalies over the WNP. The anomalous southwesterly over the northwestern edge of the anticyclonic flow advected the warm-moist air from the equator to increase the rainfall over East Asia. This can be interpreted as the occurrence of the Changma, which

denotes a monsoonal precipitation over Korea, along with the northward expansion of the WNP high (J. Y. Lee et al., 2017).

Simultaneously, large-scale negative precipitation anomalies also appear over the subtropical WNP, which are closely associated with local anticyclone. Additionally, negative precipitation anomalies are observed over the equatorial central Pacific, east of 150° E. This indicates the development of the La Niña event during the summer of 2020 (Zheng et al., 2021).

In the GloSea5 forecast, the simulated precipitation anomalies over Korea exhibited weaker amplitudes than the observed, and even show negative values. This is related to the weak amplitude with limited northward expansion of the clockwise streamfunction anomalies over the WNP. For example, the amplitude of the positive streamfunction anomalies over the WNP is only approximately 40% of that observed, and the latitudinal center is located far south than the observed. This indicates that the weak and southward-shifted WNP high leads to insufficient moisture advection to East Asia, and thereby fails to simulate positive rainfall anomalies over East Asia. This is consistent with the current status of the forecast ability of precipitation anomalies, which is quite low over the mid-latitudes (Figure S2).

The forecast errors in predicting the mid-latitude climate variability can originate by at least three factors: errors in (1) large-scale forcings, (2) teleconnection patterns led by large-scale forcings, (3) local internal variability. Here, we will focus on the model errors led by factor 1 and 2, as the local internal variability (i.e., factor 3) is largely controlled by the synoptic/mesoscale weather variability, which is unpredictable on a seasonal timescale (Lorenz, 1969).

To isolate the forecast errors associated with factor 2 from factor 1, we conducted a series of sensitivity tests using a partial nudging technique. By prescribing the observed SST over the IO or equatorial central eastern Pacific (EqPac), we eliminated a portion of forecast errors in predicting the extreme rainfall in the summer of 2020 by the error in tropical SST forcing. Notably, the total SST values were prescribed for the partial nudging experiment, and the impact of the observed SST anomalies was obtained by subtracting the results from control partial nudging experiments using the climatological SST forcing over either IO or EqPac.

The partial nudging experiments using the observed tropical IO (IO OBS SST) and equatorial Pacific (EqPac OBS SST) significantly improved the simulation quality of the monsoon rainfall in summer 2020 (Figure 2). The amplitudes of positive precipitation anomalies averaged from July 1 to August 12 in IO OBS SST and EqPac OBS SST were 0.5, and 1.0 mm/day, respectively (black bars in Figure 2a). Consequently, the summed amplitude of the precipiation anomaly over East Asia after prescribing the observed IO and EqPac SST is increased to 1.5 mm/day, which is approximately 40% of the observed amount (i.e., 3.5 mm/day).

The spatial distribution of the summed precipitation and streamfunction anomalies in two partial nudging experiments (i.e., IO OBS SST and EqPac OBS SST experiments) were also similar to those observed (Figure 2b). The amplitude of the positive streamfunction anomaly over the subtropical WNP is increased about 50% compared to that in the operational forecasts in Figure 1d. Also the negative precipitation anomalies over the subtropical WNP become prominent in the partial nudging experiments. Rainbands over Korea, Japan, and northern China are located over the northern part of the WNP anticyclonic flow in partial nudging experiments. This indicates that GloSea5 simulates a realistic teleconnection pattern with the corrected warm IO SST and the La Nina-related SST.

One can wonder whether the summed responses of IO and EqPac experiments would be different from the results of a single nudging experiment that both IO and EqPac SST are prescribed. This nonlinearity of the atmospheric response may be worthwhile to be considered, however, we here argue that the linear assumption in the atmospheric responses to tropical SST forcing is also valid to some extent. This can be supported by the wide usage of the linearized model to investigate the atmospheric response to the tropical SST forcing (Annamalai et al., 2010; Watanabe & Jin, 2003). In this sense, we believe that the overall response of a nudging experiment with both IO and EqPac SST is not essentially different from that of summed response of IO and EqPac experiments.

Note that the latitudinal center of the WNP anticyclone is still located to the south of 20°N in the partial nudging experiments (Figure 2b), whereby it is located at 30°N in the observation (Figure 1c). This can be one reason that the rainfall anomalies over East Asia is still underestimated in GloSea5. In addition, the

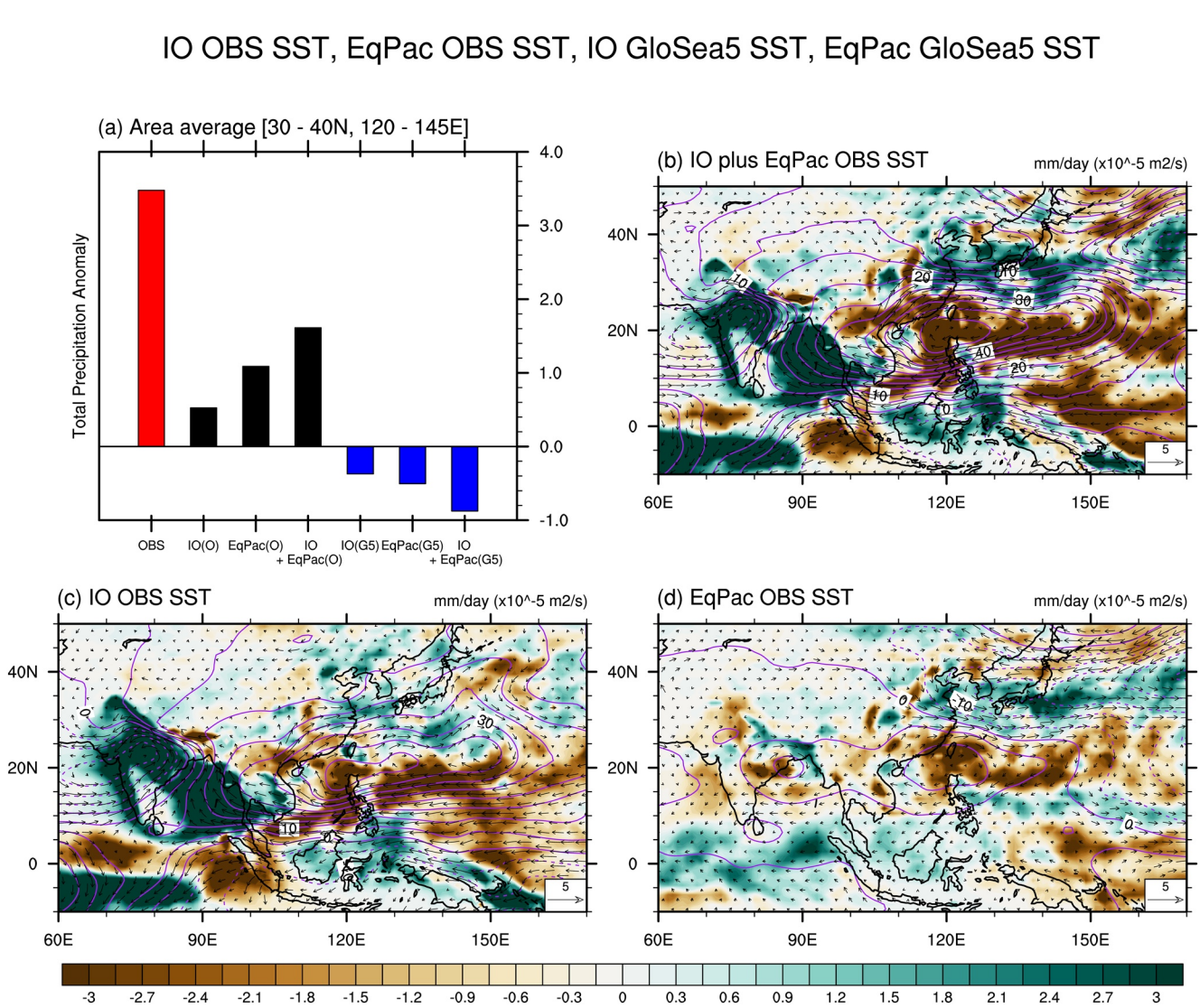

Figure 2. (a) East Asian precipitation anomaly, defined as the area-averaged value over 30°–40°N, 120°–145°E, in the observation and results of each experiment (observation-red bar, IO(O)-first black bar, EqPac(O)-second black bar, IO + EqPac-third black bar, IO(G5)-first blue bar, EqPac(G5)-second blue bar, and IO(G5)+EqPac(G5)-third blue bar). The spatial distribution of the precipitation (shading), 850 hPa streamfunction (contour), and wind-vector anomalies (vector) in (b) the summed anomalies in IO OBS SST and EqPac OBS SST experiments, (c) IO OBS sea surface temperature (SST), and (d) EqPac OBS SST experiments. Notably, the partial nudging area for IO OBS SST and EqPac OBS SST is 20°S–20°N, 40°–100°E, and 20°S–20°N, 180°–75°W respectively.

observed negative precipitation anomalies over the South Asia including India are still not simulated in the partial nudging experiments, implying that the intrinsic model errors still cause the systematic forecast errors over some regions even after correcting the SST.

In IO OBS SST experiment, the dipole precipitation anomalies over the northern IO and the subtropical WNP are prominent (Figure 2c). This indicates that the GloSea5 successfully simulates the IO capacitor effect: IO SST warming increases the local precipitation anomalies around the northern part (Kosaka et al., 2013; Xie et al., 2016), which acts as an atmospheric heating to induces the frictional divergence over the low-tropospheric subtropical WNP (Kosaka et al., 2021; Xie et al., 2009). As a result, atmospheric convections are suppressed over the subtropical WNP to induce the WNP high.

In EqPac OBS SST experiment, the negative equatorial precipitation anomalies are shown at the east of 150°E due to the La Nina SST forcing (Figure 2d). The negative precipitation anomalies lead the anticyclonic Gill-type Rossby wave response over the subtropical WNP (Gill, 1980). Also, it can excite a meridional

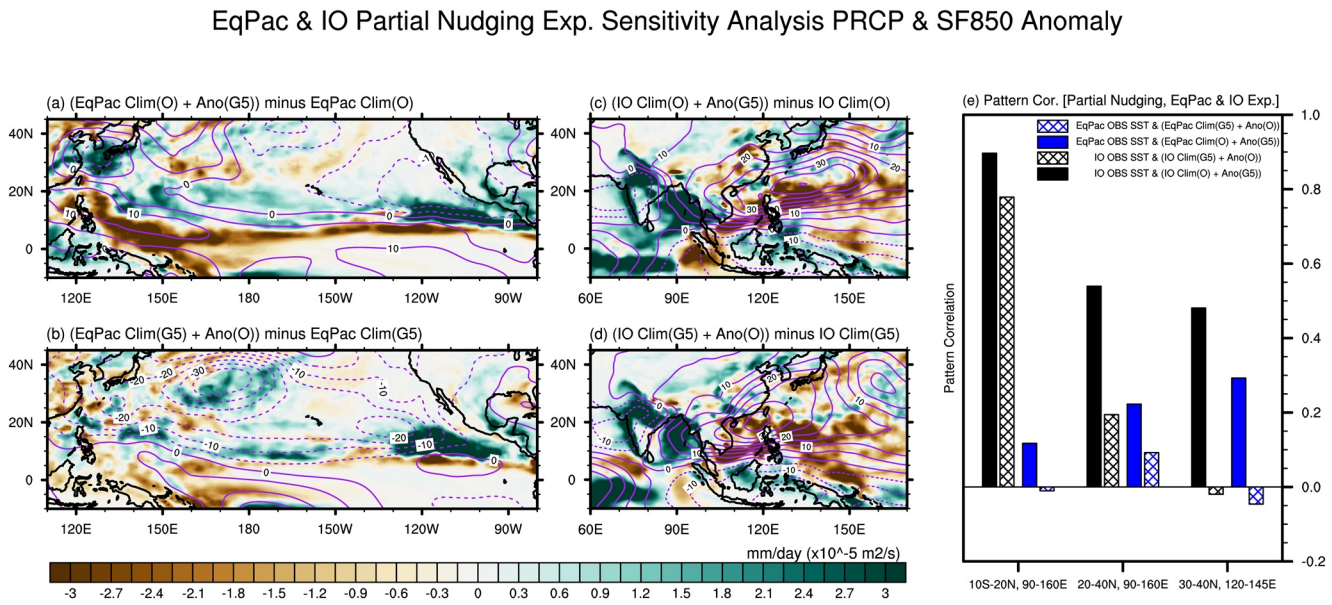

Figure 3. The precipitation (shading) and 850 hPa streamfunction (contour) anomalies averaged during July 1 to August 12, 2020 in the (a) "EqPac Clim(O) + Ano(G5)", (b) "EqPac Clim(G5) + Ano(O)", (c) "IO Clim(O) + Ano(G5)", and (d) "IO Clim(G5) + Ano(O)" experiments. (e) The pattern correlation of the precipitation anomalies in the partial nudging experiment using the observed total IO SST and that in the "IO Clim(O) + Ano(G5)" (black filled bar), "IO Clim(G5) + Ano(O)" (black checked bar), "EqPac Clim(O) + Ano(G5)" (blue filled bar), "EqPac Clim(G5) + Ano(O)" (blue checked bar) sensitivity experiment in various East Asian domains.

wave train propagating northward to Korea and Japan, which resembles Pacific–Japan (PJ) teleconnection pattern (Nitta, 1987).

To confirm that the tropical SST pattern is responsible for the simulation quality of the monsoon rainfall over East Asia, another set of partial nudging experiments was conducted by prescribing the forecasted SST over the IO or EqPac (Figure S3). The results show that the forecasted SST does not successfully mimic the observed rainfall anomalies over East Asia and the associated circulation anomalies (blue bars in Figure 2a). Moreover, the anomalous anticyclonic flow over the WNP does not extend to north of 20° N (Figures S3a and S3b), which is consistent with the operational GloSea5 forecasts (Figure 1d). This confirms that the forecast error in the tropical SST anomalies is the primary reason for the systematic underestimation of rainfall anomalies over East Asia in the summer of 2020.

4. Role of Climatological Fields in Simulating Extreme Rainfall Events

The differences between the observed and forecasted SST used for the partial nudging experiments can be attributed to two SST components: climatological and anomalous components. In this section, we demonstrate that the errors in climatological fields are critical in the simulation quality of extreme rainfall events over East Asia.

Additional partial nudging experiments were conducted by prescribing the equatorial Pacific SST whose climatological was obtained from observation but the anomalous component was obtained from the GloSea5 forecast (i.e., "EqPac Clim(O) + Ano(G5)" exp.). Partial nudging experiments with the GloSea5 climatological SST and observed SST anomalies (i.e., "EqPac Clim(G5) + Ano(O)" exp.) are compared. The anomalous precipitation and circulation responses were obtained by subtracting the results from the partial nudging experiments using the corresponding climatological fields.

Figure 3a shows the precipitation anomalies in the "EqPac Clim(O) + Ano(G5)" experiment. Positive precipitation anomalies were successfully simulated over East Asia. The negative precipitation anomalies that indicate the development of anticyclone anomalies over the WNP were also clear, as shown in the EqPac OBS SST experiments (Figure 2d). This implies that the overall precipitation responses did not change significantly when the prescribed SST anomalies were obtained from either the observations or forecasts.

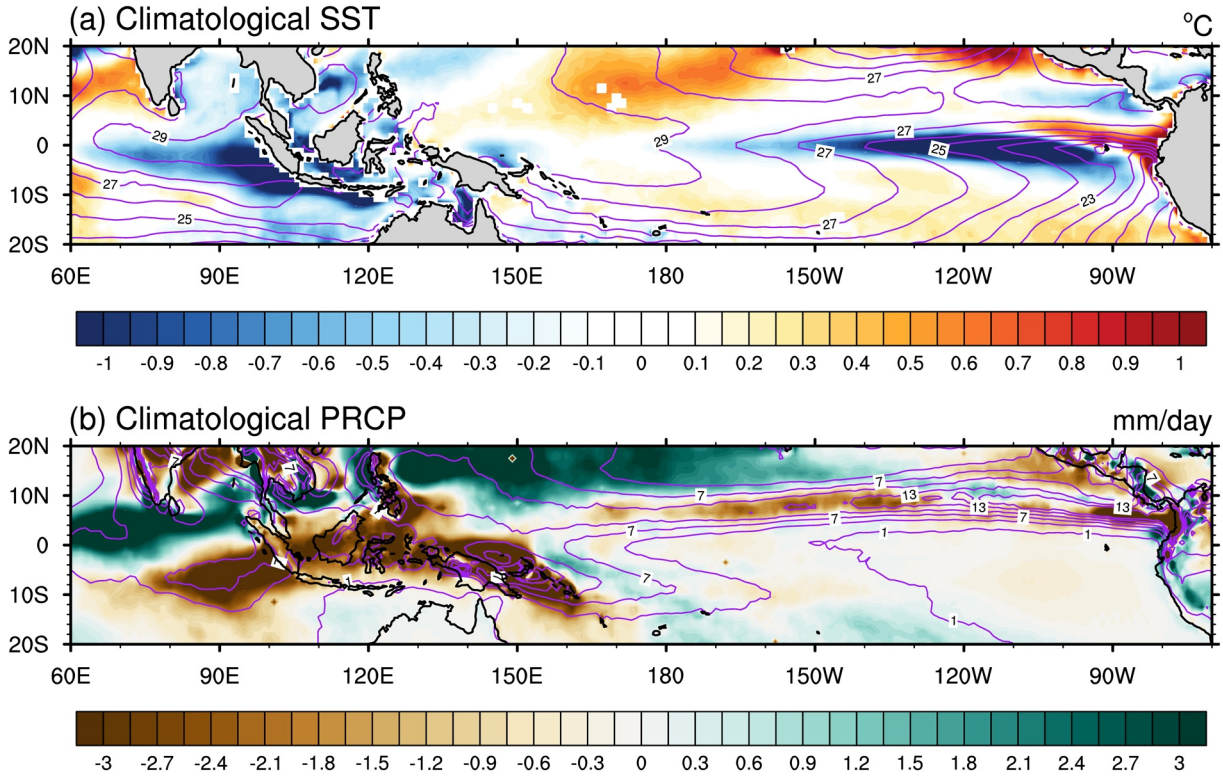

Figure 4. Climatological bias (GloSea5-observation) of the (a) sea surface temperature (SST) and (b) precipitation. In panels (a) and (b), the shading indicates the climatological bias between the GloSea5 hindcast and observation, and the contour indicates the climatology of observation. Note that the climatological precipitation in GloSea5 is shown after the Cumulative Distribution Function (CDF) matching to the observed.

Therefore, the forecast errors in the equatorial Pacific SST anomalies are not responsible for the systematic underestimation of rainfall anomalies over East Asia.

Conversely, the overall precipitation response changes dramatically once the climatological fields change to the forecasted. Figure 3b shows that the overall precipitation response become weak in the "EqPac Clim(G5) + Ano(O)" experiment. In addition to the precipitation anomalies over East Asia, the negative precipitation anomalies over the equatorial Pacific were systematically weakened. Additionally, the stream-function anomalies over the WNP exhibited even negative values, which is in contrast to the observed. This indicates that the precipitation anomalies during identical SST anomalies are strongly dependent on the background SST.

Consequently, the pattern correlation of the precipitation anomalies between the partial nudging experiment and the observed total SST over the equatorial central eastern Pacific is generally higher in the "EqPac Clim(O) + Ano(G5)" experiment over East Asia (Figure 3b). This demonstrates the critical role of the equatorial climatological SST in simulating anomalous atmospheric responses over East Asia and the equatorial region.

The role of climatological fields in the forecasting skill over East Asia is also crucial in the IO region. In the "IO Clim(O) + Ano(G5)" experiment, the positive precipitation anomalies were evident over Korea and Japan (Figure 3c). The anticyclonic flows over the WNP exhibited similar spatial structures and amplitudes to those in the IO OBS SST experiment (Figure 2c). Conversely, the precipitation anomalies over East Asia showed negative values in the "IO Clim(G5) + Ano(O)" experiment, and the horizontal scale of the WNP high was not large as that observed (Figure 3d). This is supported by the pattern correlation of the precipitation anomalies, which is higher in the "IO Clim(O) + Ano(G5)" experiment (Figure 3c).

It is natural to ask which aspect of climatological SST is responsible for the systematic errors of the anomalous precipitation response in GloSea5. Figure 4a shows the climatological SST bias averaged from July 1

to August 12, 2020 in the observation and GloSea5 data. The most prominent feature is the cold SST bias over the equatorial eastern Pacific and the eastern IO. The SST biases over the EqPac and tropical eastern IO reached −1°C . Notably, the cold bias over the equatorial cold tongue region is common in several climate models (Ham et al., 2010; Li & Xie, 2014). Although not highlighted in this study, a warm SST biases were also found over the subtropical WNP and equatorial western IO with a weaker amplitude than that of the cold bias.

Subsequently, we compared the climatological precipitation bias. The area-averaged precipitation amount over the tropical Indo-Pacific region (20° S–20° N, 40°E−70°W) is overestimated in the GloSea5 (4.89 mm/day) compared to that observed (4.63 mm/day), even though the climatological SST is similar to each other (i.e., 27.08°C and 27.03°C in the GloSea5 and observation, respectively). This indicates that the overestimation of the precipitation amount could be attributed to the imperfection of the convective parameterization. This also implies that the tropical-averaged precipitation bias would not be significantly related to the precipitation anomaly, as uniform atmospheric heating does not contribute to the convection anomaly by increasing the convective threshold (Chou et al., 2009; Johnson & Xie, 2010). Therefore, to remove the tropical mean component of the precipitation bias, cumulative distribution function (CDF) matching was applied to the climatological precipitation in the GloSea5 (H. Li et al., 2010; Yang et al., 2018). The observed and GloSea5 climatological precipitation at each grid point within 20° S–20° N and 40°E−70°W are sorted in the amplitude order. Subsequently, the values in GloSea5 with a specific quantile is changed to the observed of the corresponding quantile. The tropical mean precipitation bias was removed through CDF matching, and the climatological precipitation bias at any specific region was more closely related to that in the SST and the resultant precipitation anomaly.

Figure 4b shows the tropical climatological precipitation bias in the GloSea5 forecasts after CDF matching. Over the equatorial eastern Pacific or tropical eastern IO, where the cold SST bias is located, the climatological convective activity in GloSea5 tends to be weaker than that observed (i.e., dry bias). The precipitation bias over the equatorial eastern Pacific (5°–10°N, 180°–90°W) is −1.38 mm/day, and that of the tropical eastern IO (10°–0°S, 90°–110°E) is approximately −2.9 mm/day. Wet bias (i.e., excessive convective activities) over the subtropical western Pacific and equatorial western IO lead the downward motion over the adjacent regions to compensate for the local upward motion (Watanabe & Jin, 2003), which can further suppress the convective activity and reduce the resultant precipitation over the equatorial eastern Pacific and eastern IO. Note that the overall sign of the precipitation bias does not change significantly without CDF matching, even though the amplitude of the dry bias is reduced (Figure 4).

The dry bias over the equatorial eastern Pacific and eastern IO is responsible for the weaker convective activity anomalies to the given SST forcing (Cai et al., 2014; Ham & Kug, 2012, 2015; Kug et al., 2011, 2012; Watanabe et al., 2011). Owing to the cold SST bias over the equatorial eastern Pacific, the climatological downward motion in GloSea5 is greater than that observed, and consequently, the anomalous upward motion by the given positive SST anomalies can barely overcome the climatological downward motion. Therefore, the precipitation anomalies are hardly induced as the total vertical motion still exhibits a downward direction. This is confirmed by the precipitation anomalies regressed onto the northern IO SST anomalies (i.e., SST averaged over 10°S−20°N, 90°–110°E), indicating the precipitation response is generally weaker in GloSea5 (i.e., 1.34 mm/day/°C for observation, and 0.80 mm/day/°C for GloSea5). Similarly, the precipitation anomalies by Nino3.4 (5°S–5°N, 170°–120°W) SST anomaly are systematically weaker in GloSea5 than the observation (i.e., 1.58 mm/day/°C for observation, and 0.92 mm/day/°C for GloSea5). The weakened local convection anomalies attenuate the precipitation response over the subtropical WNP in GloSea5, confirming that the cold and dry climatological bias in GloSea5 is responsible for the weakened tropical atmospheric responses to the SST forcing. Therefore, tropical climatological bias significantly affects the seasonal forecast skill over the mid-latitudes by modulating the atmospheric teleconnection patterns.

5. Summary and Conclusions

This study examined the origin of the forecast errors of GloSea5, the operational seasonal forecast system in KMA, in predicting heavy rainfall in 2020 summer over East Asia. The precipitation anomalies over East Asia, covering Korea, Japan, and northern China during July to early August, 2020 were significantly

underestimated in the GloSea5 operational forecasts. This error has partly been attributed to a weaker northward expansion of the WNP subtropical high.

Through a series of partial nudging experiments, we found that the East Asian monsoon rainfall anomalies can be successfully predicted by GloSea5 when the tropical SST forcing is corrected. Once the observed total SST was applied over the IO and tropical central eastern Pacific, the northern edge of the anticyclonic flow anomalies over the subtropical western Pacific well extended to East Asia; this transports warm-moist air from the tropics to the region. Consequently, the simulated positive precipitation anomalies over East Asia in the partial nudging experiments using the observed IO and equatorial Pacific SST increased up to approximately 40% of that observed.

We further found that the climatological SST and associated convective activity are crucial in simulating the amplitude of the WNP high and the resultant East Asian precipitation anomalies in the summer of 2020. Namely, the simulated precipitation anomalies over East Asia exhibited a positive value only in partial nudging experiments using the observed SST climatology plus either the observed or GloSea5 SST anomalies, while they exhibited a negative value in the experiments using the GloSea5 climatology. According to the nonlinear SST-precipitation relationship, the cold and dry biases over the eastern Pacific and eastern IO in GloSea5 were responsible for the weakened atmospheric response to the given SST anomalies. This implies that the climatological fields are crucial in simulating the interannual variability; therefore, it affects the quality of operational seasonal forecasts.

One can wonder the possible role of Atlantic ocean warming on the heavy rainfall event in East Asia during summer 2020 (Zheng & Wang, 2021). The partial nudging experiments by prescribing the forecasted SST over Atlantic using GloSea5 showed the increase in the precipitation over the northern China, Korea, and Japan (Figure S5), indicating the role of Atlantic SST. However, as the precipitation increase with the Atlantic SST is well simulated with the forecasted SST, we focus on the Indo-Pacific SST to examine on the origin of the forecast error to SST.

This study proposes an alternative experimental design to improve the seasonal forecast skills, which can be utilized in operational sense. After the operational forecasts are generated, additional nudging experiments can be conducted by replacing the climatological SST. Namely, partial nudging experiments using the observed climatology and forecasted anomalies (e.g., a type of Clim(O) + Ano(G5) in this study) can be conducted in the operational mode, which would improve the East Asian seasonal forecast skill by correcting the background states. This study also suggests that a proper evaluation of the climatological fields in operational forecasts is necessary to improve the seasonal forecast skills.

Data Availability Statement

The European Centre for Medium-Range Weather Forecasts (ECMWF) provided the fifth generation of ECMWF reanalysis (ERA5, https://www.ecmwf.int/en/forecasts/datasets/reanalysis-datasets/era5). The National Oceanic and Atmospheric Administration (NOAA) provides the Optimum Interpolation SST version 2 (OISST v.2, https://www.ncdc.noaa.gov/oisst/optimum-interpolation-sea-surface-temperature-oisst-v20) and Global Precipitation Climatology Project (GPCP) version 2 (GPCP v.2, https://psl.noaa.gov/data/gridded/data.gpcp.html).

Acknowledgments
This study was supported by the Korea Meteorological Administration Research and Development Program under Grant KMI2021-01210. T. Li was jointly supported by NSFC grant 42088101, and NSF AGS-2006553.

References

Adler, R. F., Huffman, G. J., Chang, A., Ferraro, R., Xie, P. P., Janowiak, J., et al. (2003). The version-2 global precipitation climatology project (GPCP) monthly precipitation analysis (1979–present). *Journal of Hydrometeorology*, *4*(6), 1147–1167. https://doi.org/10.1175/1525-7541(2003)004<1147:tvgpcp>2.0.co;2

Annamalai, H., Kida, S., & Hafner, J. (2010). Potential impact of the tropical Indian Ocean–Indonesian seas on El Niño characteristics. *Journal of Climate*, *23*(14), 3933–3952. https://doi.org/10.1175/2010jcli3396.1

Bowler, N. E., Arribas, A., Beare, S. E., Mylne, K. R., & Shutts, G. J. (2009). The local ETKF and SKEB: Upgrades to the MOGREPS short-range ensemble prediction system. *Quarterly Journal of the Royal Meteorological Society: A journal of the atmospheric sciences, applied meteorology and physical oceanography*, *135*(640), 767–776. https://doi.org/10.1002/qj.394

Cai, W., Borlace, S., Lengaigne, M., Van Rensch, P., Collins, M., Vecchi, G., et al. (2014). Increasing frequency of extreme El Niño events due to greenhouse warming. *Nature Climate Change*, *4*(2), 111–116. https://doi.org/10.1038/nclimate2100

Chikamoto, Y., Mochizuki, T., Timmermann, A., Kimoto, M., & Watanabe, M. (2016). Potential tropical Atlantic impacts on Pacific decadal climate trends. *Geophysical Research Letters*, *43*(13), 7143–7151. https://doi.org/10.1002/2016gl069544

Chou, C., Neelin, J. D., Chen, C. A., & Tu, J. Y. (2009). Evaluating the "rich-get-richer" mechanism in tropical precipitation change under global warming. *Journal of Climate*, *22*(8), 1982–2005. https://doi.org/10.1175/2008jcli2471.1

Gill, A. E. (1980). Some simple solutions for heat-induced tropical circulation. *Quarterly Journal of the Royal Meteorological Society*, *106*(449), 447–462. https://doi.org/10.1002/qj.49710644905

Ham, Y. G., Chikamoto, Y., Kug, J. S., Kimoto, M., & Mochizuki, T. (2017). Tropical Atlantic-Korea teleconnection pattern during boreal summer season. *Climate Dynamics*, *49*(7), 2649–2664. https://doi.org/10.1007/s00382-016-3474-z

Ham, Y. G., & Kug, J. S. (2012). How well do current climate models simulate two types of El Niño? *Climate Dynamics*, *39*(1–2), 383–398. https://doi.org/10.1007/s00382-011-1157-3

Ham, Y. G., & Kug, J. S. (2015). Improvement of ENSO simulation based on intermodel diversity. *Journal of Climate*, *28*(3), 998–1015. https://doi.org/10.1175/jcli-d-14-00376.1

Ham, Y. G., Kug, J. S., & Kang, I. S. (2007). Role of moist energy advection in formulating anomalous Walker circulation associated with El Niño. *Journal of Geophysical Research*, *112*(D24). https://doi.org/10.1029/2007jd008744

Ham, Y. G., Kug, J. S., Kang, I. S., Jin, F. F., & Timmermann, A. (2010). Impact of diurnal atmosphere–ocean coupling on tropical climate simulations using a coupled GCM. *Climate Dynamics*, *34*(6), 905–917. https://doi.org/10.1007/s00382-009-0586-8

Ham, Y. G., Kug, J. S., Park, J. Y., & Jin, F. F. (2013). Sea surface temperature in the north tropical Atlantic as a trigger for El Niño/Southern Oscillation events. *Nature Geoscience*, *6*(2), 112–116. https://doi.org/10.1038/ngeo1686

Hersbach, H., Bell, B., Berrisford, P., Hirahara, S., Horányi, A., Muñoz-Sabater, J., et al. (2020). The ERA5 global reanalysis. *Quarterly Journal of the Royal Meteorological Society*, *146*(730), 1999–2049. https://doi.org/10.1002/qj.3803

Johnson, N. C., & Xie, S. P. (2010). Changes in the sea surface temperature threshold for tropical convection. *Nature Geoscience*, *3*(12), 842–845. https://doi.org/10.1038/ngeo1008

Kosaka, Y., Takaya, Y., & Kamae, Y. (2021). The Indo-western Pacific Ocean capacitor effect. *Tropical and Extratropical Air-Sea Interactions*, 141–169. https://doi.org/10.1016/b978-0-12-818156-0.00012-5

Kosaka, Y., Xie, S. P., Lau, N. C., & Vecchi, G. A. (2013). Origin of seasonal predictability for summer climate over the Northwestern Pacific. *Proceedings of the National Academy of Sciences*, *110*(19), 7574–7579. https://doi.org/10.1073/pnas.1215582110

Kug, J. S., Ham, Y. G., Lee, J. Y., & Jin, F. F. (2012). Improved simulation of two types of El Niño in CMIP5 models. *Environmental Research Letters*, *7*(3), 034002. https://doi.org/10.1088/1748-9326/7/3/034002

Kug, J. S., Sooraj, K. P., Jin, F. F., Ham, Y. G., & Kim, D. (2011). A possible mechanism for El Niño-like warming in response to the future greenhouse warming. *International Journal of Climatology*, *31*(10), 1567–1572. https://doi.org/10.1002/joc.2163

Lee, E. J., Yeh, S. W., Jhun, J. G., & Moon, B. K. (2006). Seasonal change in anomalous WNPSH associated with the strong East Asian summer monsoon. *Geophysical Research Letters*, *33*(21). https://doi.org/10.1029/2006gl027474

Lee, J. Y., Kwon, M., Yun, K. S., Min, S. K., Park, I. H., Ham, Y. G., et al.(2017). The long-term variability of Changma in the East Asian summer monsoon system: A review and revisit. *Asia-Pacific Journal of Atmospheric Sciences*, *53*(2), 257–272. https://doi.org/10.1007/s13143-017-0032-5

Lee, S. J., Hyun, Y. K., Lee, S. M., Hwang, S. O., Lee, J., & Boo, K. O. (2020). Prediction skill for East Asian summer monsoon indices in a KMA global seasonal forecasting system (GloSea5). *Atmosphere*, *30*(3), 293–309. (In Korean).

Li, G., & Xie, S. P. (2014). Tropical biases in CMIP5 multimodel ensemble: The excessive equatorial Pacific cold tongue and double ITCZ problems. *Journal of Climate*, *27*(4), 1765–1780. https://doi.org/10.1175/jcli-d-13-00337.1

Li, H., Sheffield, J., & Wood, E. F. (2010). Bias correction of monthly precipitation and temperature fields from intergovernmental panel on climate change AR4 models using equidistant quantile matching. *Journal of Geophysical Research*, *115*(D10). https://doi.org/10.1029/2009jd012882

Li, T., Wang, B., Wu, B., Zhou, T. J., Chang, C. P., & Zhang, R. H. (2017). Theories on formation of an anomalous anticyclone in Western North Pacific during El Niño: A review. *Journal of Meteorological Research*, *31*(6), 987–1006. https://doi.org/10.1007/s13351-017-7147-6

Lorenz, E. N. (1969). Atmospheric predictability as revealed by naturally occurring analogues. *Journal of the Atmospheric Sciences*, *26*(4), 636–646. https://doi.org/10.1175/1520-0469(1969)26<636:aparbn>2.0.co;2

MacLachlan, C., Arribas, A., Peterson, K. A., Maidens, A., Fereday, D., Scaife, A. A., et al. (2015). Description of GloSea5: The Met Office high resolution seasonal forecast system. *Quarterly Journal of the Royal Meteorological Society*, *141*(689):1072–1084. https://doi.org/10.1002/qj.2396

Nitta, T. (1987). Convection activities in the tropical western Pacific and their impact on the Northern Hemisphere circulation. *J. Meteor. Soc. Japan*, *67*, 375–383.

Pan, X., Li, T., Sun, Y., & Zhu, Z. (2021). Cause of extreme heavy and persistent rainfall over Yangtze River in summer 2020. *Advances in Atmospheric Sciences*, https://doi.org/10.1007/s00376-021-0433-3

Park, C., Son, S. W., Kim, H., Ham, Y. G., Kim, J., Cha, D. H., et al. (2021). Record-breaking summer rainfall in South Korea in 2020: Synoptic characteristics and the role of large-scale circulations. *Monthly Weather Review*. https://doi.org/10.1175/MWR-D-21-0051.1

Park, S., Kim, D. J., Lee, S. W., Lee, K. W., Kim, J., Song, E. J., & Seo, K. H. (2017). Comparison of extended medium-range forecast skill between KMA ensemble, ocean coupled ensemble, and GloSea5. *Asia-Pacific Journal of Atmospheric Sciences*, *53*(3), 393–401. https://doi.org/10.1007/s13143-017-0035-2

Reynolds, R. W., Smith, T. M., Liu, C., Chelton, D. B., Casey, K. S., & Schlax, M. G. (2007). Daily high-resolution-blended analyses for sea surface temperature. *Journal of Climate*, *20*(22), 5473–5496. https://doi.org/10.1175/2007jcli1824.1

Wang, B., Wu, R., & Li, T. I. M. (2003). Atmosphere–warm ocean interaction and its impacts on Asian–Australian monsoon variation. *Journal of Climate*, *16*(8), 1195–1211. https://doi.org/10.1175/1520-0442(2003)16<1195:aoiaii>2.0.co;2

Wang, B., & Zhang, Q. (2002). Pacific–east Asian teleconnection. Part II: How the Philippine Sea anomalous anticyclone is established during El Nino development. *Journal of Climate*, *15*(22), 3252–3265. https://doi.org/10.1175/1520-0442(2002)015<3252:peatpi>2.0.co;2

Watanabe, M., Chikira, M., Imada, Y., & Kimoto, M. (2011). Convective control of ENSO simulated in MIROC. *Journal of Climate*, *24*(2), 543–562. https://doi.org/10.1175/2010JCLI3878.1

Watanabe, M., & Jin, F. F. (2003). A moist linear baroclinic model: Coupled dynamical–convective response to El Niño. *Journal of Climate*, *16*(8), 1121–1139. https://doi.org/10.1175/1520-0442(2003)16<1121:amlbmc>2.0.co;2

Wu, B., Zhou, T., & Li, T. (2009). Seasonally evolving dominant interannual variability mode over the East Asia. *Journal of Climate*, *22*, 2992–3005. https://doi.org/10.1175/2008jcli2710.1

Wu, B., Zhou, T., & Li, T. (2017a). Atmospheric dynamic and thermodynamic processes driving the western North Pacific anomalous anticyclone during El Niño. Part I: Maintenance mechanisms. *Journal of Climate*, *30*, 9621–9635. https://doi.org/10.1175/jcli-d-16-0489.1

Wu, B., Zhou, T., & Li, T. (2017b). Atmospheric dynamic and thermodynamic processes driving the western North Pacific anomalous anticyclone during El Niño. Part II: Formation processes. *Journal of Climate*, *30*, 9637–9650. https://doi.org/10.1175/jcli-d-16-0495.1

Wu, Y., Tang, C., & Dunlap, E. (2010). Assimilation of sea surface temperature into CECOM by flux correction. *Ocean Dynamics*, *60*(2), 403–412. https://doi.org/10.1007/s10236-010-0266-6

Xie, S. P., Hu, K., Hafner, J., Tokinaga, H., Du, Y., Huang, G., & Sampe, T. (2009). Indian Ocean capacitor effect on Indo–western Pacific climate during the summer following El Niño. *Journal of Climate*, *22*(3), 730–747. https://doi.org/10.1175/2008jcli2544.1

Xie, S. P., Kosaka, Y., Du, Y., Hu, K., Chowdary, J. S., & Huang, G. (2016). Indo-western Pacific Ocean capacitor and coherent climate anomalies in post-ENSO summer: A review. *Advances in Atmospheric Sciences*, *33*(4), 411–432. https://doi.org/10.1007/s00376-015-5192-6

Yang, X., Wood, E. F., Sheffield, J., Ren, L., Zhang, M., & Wang, Y. (2018). Bias correction of historical and future simulations of precipitation and temperature for China from CMIP5 models. *Journal of Hydrometeorology*, *19*(3), 609–623. https://doi.org/10.1175/jhm-d-17-0180.1

Zhang, W., Huang, Z., Jiang, F., Stuecker, M. F., Chen, G., & Jin, F. F. (2021). Exceptionally persistent Madden-Julian Oscillation activity contributes to the extreme 2020 East Asian summer monsoon rainfall. *Geophysical Research Letters*, *48*(5), e2020GL091588. https://doi.org/10.1029/2020gl091588

Zheng, F., Yuan, Y., Ding, Y., Li, K., Fang, X., Zhao, Y., & Jia, X. (2021). The 2020/21 extremely cold winter in China influenced by the synergistic effect of La Niña and warm Arctic. *Advances in Atmospheric Sciences*.

Zheng, J. Y., & Wang, C. Z. (2021). Influences of three oceans on record-breaking rainfall over the Yangtze River Valley in June 2020. *Science China Earth Sciences*, *10*. https://doi.org/10.1007/s11430-020-9758-9